Int. J. Electrochem. Sci., 12 **(2017)** 9784 – 9797, doi: 10.20964/2017.10.75

International Journal of ELECTROCHEMICAL SCIENCE
www.electrochemsci.org

A Signal-on Electrochemiluminescence Immunosensor for Detecting Alpha Fetoprotein Using Gold Nanoparticle-Graphite-Like Carbon Nitride Nanocomposite as Signal Probe

Jiangru Wang[1], *Xinli Guo* [1], *Huijuan Li* [2], *Yucheng Jin*[1], *Lusheng Chen* [1,*], *Qi Kang* [1,*]

[1] College of Chemistry, Chemical Engineering and Materials Science, Collaborative Innovation Center of Functionalized Probes for Chemical Imaging in Universities of Shandong, Key Laboratory of Molecular and Nano Probes, Ministry of Education, Shandong Provincial Key Laboratory of Clean Production of Fine Chemicals, Shandong Normal University, Jinan 250014, P. R. China.
[2] College of Chemical and Environmental Engineering, Shandong University of Science and Technology, Qingdao, 266590, P.R.China
[*]E-mail:chls61@126.com; qikang@sdu.edu.cn

Received: 3 June 2017 / *Accepted:* 14 August 2017 / *Published:* 12 September 2017

The determination of cancer biomarkers plays an important role in early cancer screening and disease diagnosis. Herein, we designed a sandwiched "signal on" electrochemiluminescence (ECL) immunosensor to alpha fetoprotein (AFP) using gold nanoparticle-modified graphite-like carbon nitride nanosheets (Au NPs@g-C_3N_4 NSs) nanocomposite as the signal tag. The capture probes of primary antibodies were immobilized on the surface of the modified electrode of MSA–PANI/MWCNTs/GCE with high electrical conductivity. Where MSA, PANI, MWCTs, and GCE are mercaptosuccinic acid, polyaniline and multiwalled carbon nanotubes, and glass carbon electrode, respectively. The amount of AFP was quantified by the cathodic ECL of g-C_3N_4 NSs from the sandwich type immunocomplex. Under the optimized conditions, the proposed sensing strategy provides a measurable AFP concentration range from 0.1 pg mL^{-1} to 1 ng mL^{-1} with a limit of detection of 0.03 pg mL^{-1}. Such protocol exhibits high sensitivity, good stability and promising potential applications in clinical analysis.

Keywords: Electrochemiluminescence; immunosensor; graphite-like carbon nitride; alpha fetoprotein

1. INTRODUCTION

The determination of cancer biomarkers plays an important role in early cancer screening and disease diagnosis [1, 2]. Various immunoassay techniques including enzyme-linked immunosorbent assay (ELISA) and immunosensors have been developing to meet the increasing requests in sensitivity,

selectivity, speed, accuracy and automatization [3-6]. Among them, electrochemiluminescence (ECL) immunosensor offers the advantages of high sensitivity, wide dynamic response range, and simple instrumentation required [7,8]. ECL is a process whereby species electrochemically generated at the electrode surface undergo electron-transfer reactions to form excited states that emit light. The analytical performance of an ECL immunosensor depends greatly on its ECL-emitting species. Various ECL luminophores, including Ru complex, luminal and semiconductor nanomaterials have been applied to develop ECL immunosensors [9,10]. Among them, Cd series quantum dots or nanoparticles are the most frequently used semiconductor nanomaterials in ECL sensors [11,12]. However, CdSe and CdTe have raised concerns over their environmental toxicity, biocompatibility and ECL stability. Recently, carbon nanomaterials have attracted considerable attentions in developing electrochemical sensors [13,14].

Graphite-like carbon nitride (g-C_3N_4) as a metal-free semiconductor nanomaterial has typical stacked two-dimensional structure, distinct structural properties and high specific surface area [15,16]. As an organic semiconductor, g-C_3N_4 consists of only carbon and nitrogen atoms, which is environmental friendly without adverse and toxic effects. On the other hand, g-C_3N_4 can be produced cheaply on a large scale. Hence,g-C_3N_4 and its nanocomposite have been exploited widely for the applications in the fields including photocatalysts for water splitting [17-19],photoelectronic devices [20-22] and chemical sensors [23,24]. Xiao and co-worker reported the cathodic and anodic ECL behavior of g-C_3N_4 in carbon paste electrode [25,26], indicating that g-C_3N_4 is a promising ECL luminophore candidate. Since then, g-C_3N_4-based nanocomposites have been found increasing applications of in fabrication of ECL sensors to detect metallic ions [27], dopamine [28], organophosphate pesticides [29], perfluorooctanoic acid [30], cholesterol [31], cancer biomarker [32,33], cancer cells [34], and so on. Noted that most of the g-C_3N_4–based ECL sensors are in signal-off type, according to the quenching effect from the analytes. The signal-on type ECL sensors using g-C_3N_4 are scarce. For example, a signal-on ECL biosensor for detecting Con A was reported using phenoxy dextran-g-C_3N_4 as signal probe [35]. Guo and co-worker reported a potential-resolved "in-electrode" type ECL immunoassay based on functionalized g-C_3N_4 nanosheets (NSs) and Ru-NH_2 for simultaneous determination of dual targets [36]. Xu and co-worker reported a signal-on aptasensing for platelet derived growth factor based on the enhanced ECL behavior of g-C_3N_4 QDs@ g-C_3N_4 NSs [37].

In this work, we designed a sandwiched "signal on" ECL immunosensor using Au NPs@g-C_3N_4 NSs as the signal tag. Alpha fetoprotein (AFP) was chosen as the model analyte, because AFP is a plasma protein produced by the yolk sac and the liver during fetal life. An elevated AFP concentration in adult plasma is widely considered as an early indication of hepatocellular carcinoma or endodermal sinus tumor. Figure 1 shows the schematic illustration of the ECL immunosensor toward target AFP. In this strategy, the capture probes of primary antibodies (Ab_1) were immobilized on the surface of glass carbon electrode (GCE) modified by MSA–PANI/MWCNTs, where MSA, PANI and MWCNTs are mercaptosuccinic acid, polyaniline and multiwalled carbon nanotubes, respectively. The electrode of MSA–PANI/MWCNTs was chosen because it has high electrical conductivity [38] and abundant carboxyl groups for Ab_1 immobilization. The amount of AFP was quantified by the cathodic ECL of g-C_3N_4 NSs in the sandwich type immunocomplex. Under the

optimized experimental conditions, the proposed sensing strategy provides a measurable concentration of AFP range from 0.1 pg mL^{-1} to 1 ng mL^{-1} with a limit of detection (LOD) of 0.03 pg mL^{-1}. Such protocol exhibits high sensitivity, good stability and promising applications in clinical analysis.

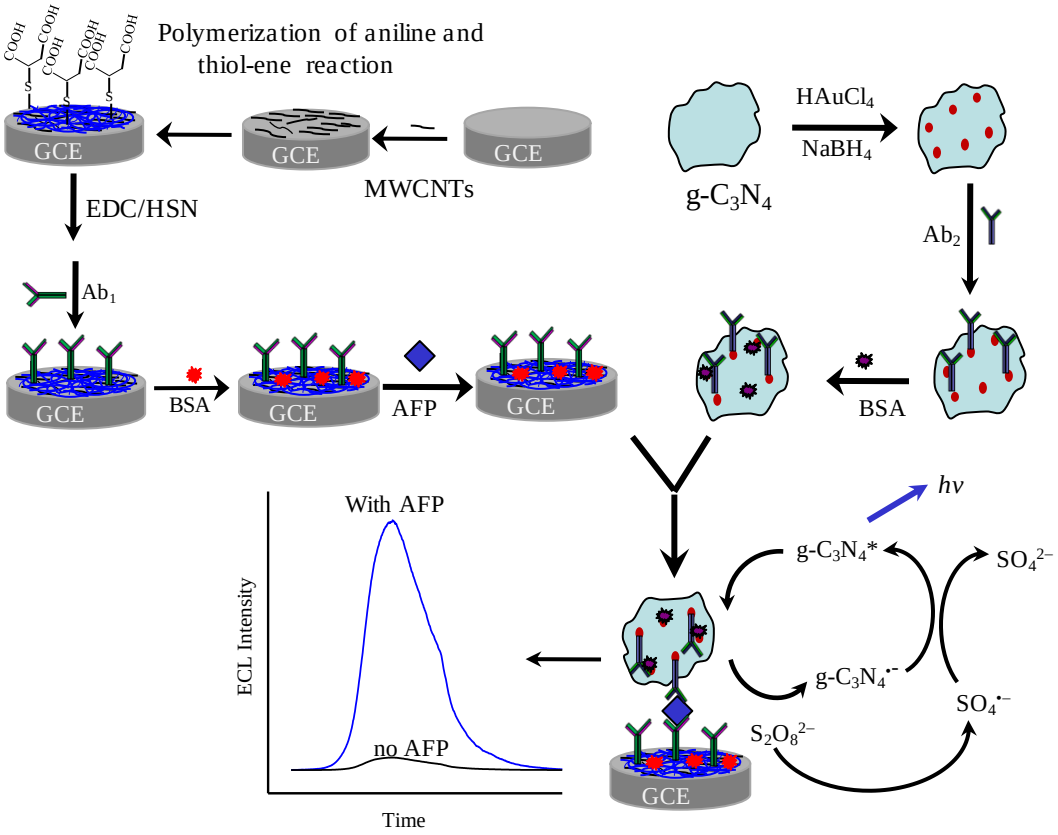

Figure 1. Schematic illustration of the preparation of the ECL immunosensor.

2. EXPERIMENTAL

2.1 Chemicals and instruments

Alpha-fetoprotein (AFP) ELISA Kits and carcinoembryonic antigen (CEA) were purchased from Biocell Biotechnology Co. Ltd. (Zhengzhou, China). Human IgG (hIgG) was purchased from Beijing Dingguo Biotechnology Development Center (Beijing, China). N-(3-dimethylamino-propyl)-N′-ethylcarbodiimide hydrochloride (EDC), N-hydroxysuccinimide (NHS) and bovine serum albumin (BSA) were purchased from Sigma–Aldrich (Shanghai, China). Mercaptosuccinic acid (MSA) and aniline were purchased from Alfa Aesar. Before use, aniline was freshly distilled over zinc dust under vacuum to remove the oxidation impurities and stored in a refrigerator. Carboxyl of multi-wall carbon nanotubes (MWCNTs, 10–20 nm diameter, 10–30 μm length and >95% purity) were obtained from Beijing Boyu Technology Co., Ltd. (China). All other chemicals were of analytical reagent grade, purchased from Sinopharm Chemical Reagent Co. Ltd (Shanghai, China). Ultrapure water (specific

resistance ≥18 MΩ cm) was used throughout the experiments. The washing and blocking buffer for immunoassay was 0.1 M phosphate buffer (pH 7.4) prepared by mixing the stock solutions of 0.1 M NaH_2PO_4 and 0.1 M Na_2HPO_4.

Transmission electron microscope (TEM) images were obtained from an H-800 microscope (Hitachi, Japan). The absorbance spectra were measured in a UV-1700 spectrophotometer (Shimadzu, Japan). The electrochemical impedance spectroscopy (EIS) analysis was carried out using a CHI 660E electrochemical workstation (Chenhua Instrument Company, Shanghai, China). MPI-E ECL analyzer (Xi'an Remex Analytical Instrument Co., Ltd. China) was used to record the ECL signals with the photomultiplier tube voltage set at 600 V. A conventional three-electrode system was employed during the experiment with an Ag/AgCl (sat. KCl) as reference electrode, a platinum wire as counter electrode and a modified glassy carbon electrode (GCE) as working electrode.

2.2. Preparation of the Au NPs@g-C_3N_4 NSs

Firstly, bulk g-C_3N_4 was prepared by one-step thermal-induced self-condensation of melamine under atmospheric condition [22]. Then, 1 g of bulk g-C_3N_4 powder was dispersed in 50 mL water and exfoliated under strong ultrasonication for 2 h to obtain g-C_3N_4 NSs. After adding 50 mL HNO_3, the mixture was refluxed at 125 °C for 24 h. Cooled naturally to room temperature, the resulting product was centrifuged and washed with ultrapure water until pH 7. The final product was vacuum dried at 35 °C for 12 h to obtain carboxylated g-C_3N_4 NSs.

Au NPs@g-C_3N_4 NSs was prepared according to the literature [33] with a slight modification. In brief, 10 mg g-C_3N_4 NSs was dispersed in 10 ml ultrapure water and sonicated for 30 min. Then 100 μL 0.05 M $HAuCl_4$ was added under stirring and sonicated for 30 min again. The resulting suspension was stirred in an ice bath, 250 μL of freshly-prepared 0.05 M $NaBH_4$ solution was injected quickly. The reaction mixture was stirred for 20 min to reduce the $AuCl_4^-$. Afterward, 250 μL of 0.02 M sodium citrate solution was dropped and the mixture was stirred for another 30 min. The Au NPs@g-C_3N_4 NSs nanocomposites were collected by centrifugation and washed with ultrapure water three times. Finally, the as-prepared Au NPs@g-C_3N_4 NSs nanocomposites were re-dispersed in 10 mL of ultrapure water and stored at 4 °C for further use and characterization.

2.3. Preparation of Au NPs@g-C_3N_4 NSs labeled Ab_2

1 mL of Au NPs@g-C_3N_4 NSs suspension was sonicated for 5 min, 50 μL second antibody (Ab_2, 100 μg mL^{-1}) was added. The mixture was slightly stirred at 4 °C for 12 h. The Ab_2 was adsorbed chemically on the surface of Au NP by the S-Au bond to obtain Au NPs@g-C_3N_4 NSs labeled Ab_2. The resulting Ab_2-Au NPs@g-C_3N_4 NSs were collected by centrifugation and washed with phosphate buffer. Then it was re-dispersed in 200 μL 0.1% BSA in phosphate buffer to bond the residual active site on Au NPs@g-C_3N_4 NSs, avoiding the non-specific adsorption for target antigen in immunoassay. The as-prepared Ab_2-Au NPs@g-C_3N_4 NSs was washed with phosphate buffer several times and dispersed in 1 mL phosphate buffer then stored at 4 °C for the further use.

2.4. Fabrication of the ECL immunosensor

Figure 1 displays the schematic illustration of the stepwise preparation of the ECL immunosensor. Prior to use, the GCE was polished successively with 1.0, 0.3 and 0.05 μm alumina slurry, and washed ultrasonically with dilute HNO_3, ethanol and water in sequence, dried by N_2 stream. Then 5μL carboxylic MWCNTs (0.5 mg mL^{-1} in water) was spread on the surface of GCE and dried under an infrared lamp. Subsequently, the MWCNTs/GCE was scanned between the potential of – 0.2 and 0.9 V at 50 mV s^{-1} for 4 cycles in 0.1 M aniline + 5 mM MSA + 0.2 M H_2SO_4 aqueous solution to fabricate MSA-PANI/ MWCNTs/GCE. After the washed with water and dried with N_2, the carboxylic groups on the surface of MSA-PANI/MWCNTs/GCE were activated by 20 μL of the freshly prepared mixture of EDC (100 mg mL^{-1}) + NHS(100 mg mL^{-1}) for 30 min at room temperature. Washed with PB, 20 μL of Ab_1 (10 μg mL^{-1}) was dropped onto the as-prepared electrode at 4 °C overnight to immobilize the capture probes. Afterward, 20 μL of 1% BSA solution was added to the electrode surface to block the residual active sites. Washed by phosphate buffer again, the resulting BSA/Ab_1-MSA-PANI/MWCNTs/GCE was stored at 4 °C while not in use.

2.5. The detection of AFP

The aforementioned biosensor was incubated with 15 μL of different concentrations AFP at 37 °C for 1 h to form the antigen–antibody complex, followed by washing. Then it was further incubated with the as-prepared Ab_2-Au NPs@g-C_3N_4 NSs for 1 h to achieve a sandwich configuration. After rinsing thoroughly with ultrapure water and phosphate buffer to remove the unbound Ab_2-Au NPs@g-C_3N_4 NSs, the ECL response of the modified electrode was recorded in 5 mL of phosphate buffer containing 0.10 M $(NH_4)_2S_2O_8$. The ECL intensity was used for the quantitative detection of APF. All measurements were operated at room temperature unless otherwise specified.

3. RESULTS AND DISCUSSION

3.1 Characterization of g-C_3N_4 NS and Au NPs@g-C_3N_4 NSs

In the design of a sandwich type “signal-on” ECL immunosensor, the luminophore with good solubility or dispersion in aqueous solution is desired for labeling the secondary antibody. Hence, the balk g-C_3N_4 was pre-treated by sonication and acidification to obtain carboxylic g-C_3N_4 NSs, which can improve its dispersion in aqueous solution. On the other hand, g-C_3N_4 NSs exhibits higher ECL intensity than balk g-C_3N_4 (data not shown). The carboxyl groups in the acidified g-C_3N_4 NS can be used to link Ab_2 via the well-known EDC/NHS reaction. In this work, we used Au NPs@g-C_3N_4 NSs nanocomposite as the ECL luminophore, because Au NPs play an important role in stabilizing ECL intensity of g-C_3N_4 NSs [33]. In addition, the Ab_2 can be linked to Au NPs on the surface of carboxylic g-C_3N_4 NS by S-Au bond between the protein and Au NPs.

Figure 2A shows the UV-vis absorbance spectra of g-C_3N_4 NSs and Au NPs@g-C_3N_4 NSs. Because g-C_3N_4 NSs are the principle component in the nanocomposites, the absorbance spectrum of Au NPs@g-C_3N_4 NSs is very similar to that of g-C_3N_4 NSs. But a small shoulder peak appears in the absorbance spectrum of Au NPs@g-C_3N_4 NSs. By using the g-C_3N_4 NSs suspension with equal absorbance at 305 nm as the reference in absorbance measurement, the difference in absorbance between Au NPs@g-C_3N_4 NSs and g-C_3N_4 NSs exhibits an obvious characteristic absorption peak at 520 nm (insert), which is attributed to absorbance from Au NPs. This result reveals the deposition of Au NPs on the surface of g-C_3N_4 NSs in the nanocomposites.

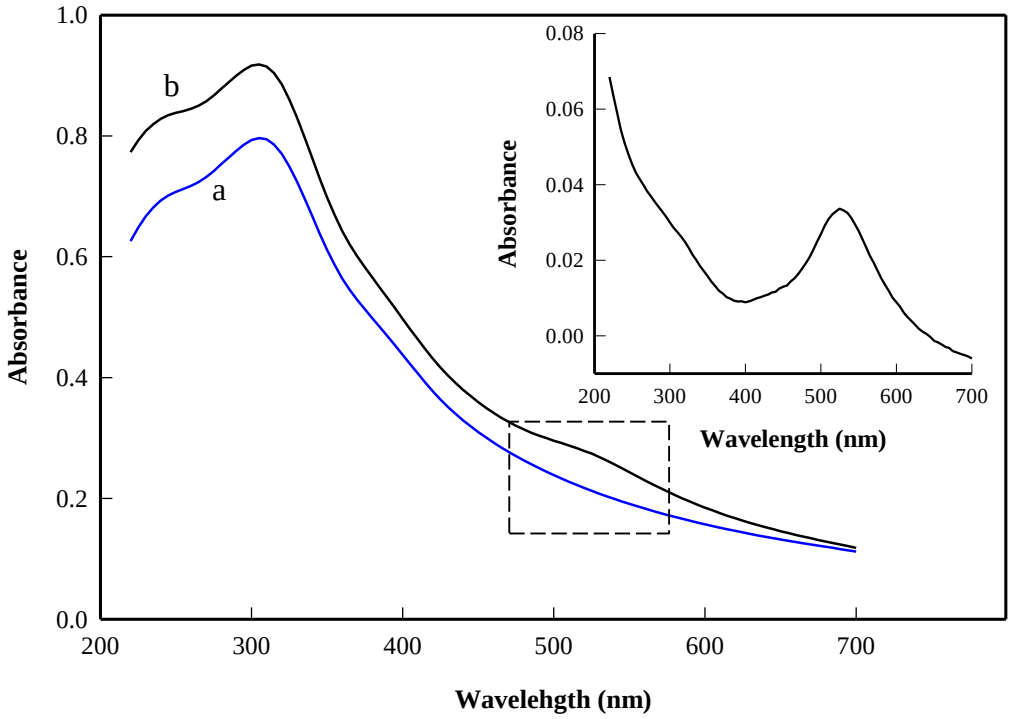

Figure 2. The UV-vis absorbance spectra of (a) g-C_3N_4 NSs (b) Au NPs@ g-C_3N_4 NSs. Insert: difference in absorbance spectrum between Au NPs@ g-C_3N_4 NSs and g-C_3N_4 NSs after data smooth algorithm

As shown in Figure 3, the as-prepared g-C_3N_4 NSs is in a two-dimensional sheet-like structure. The maximum size of the sheet is about 150 nm. Because the carboxylic groups on the surface of g-C_3N_4 provide the anchoring sites to coordinate with gold ions and promoted the reduction of $AuCl_4^-$, Au NPs (black colored dots) are uniformly distributed on the g-C_3N_4 NSs surfaces. In addition, sodium citrate can improve the dispersion stability of as-prepared Au NPs@g-C_3N_4 NSs.

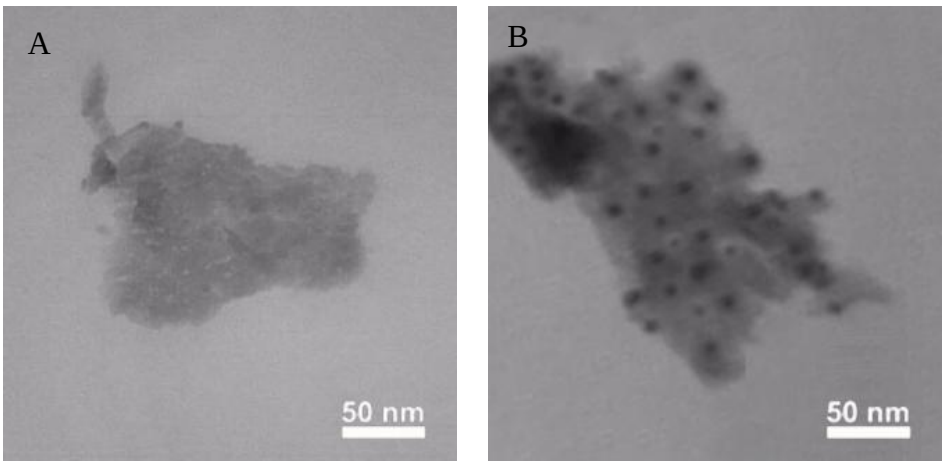

Figure 3. TEM images of (A) g-C_3N_4 nanosheets and (B) Au NPs @g-C_3N_4 nanosheets.

3.2 Electrochemical behaviors of the immunosensor

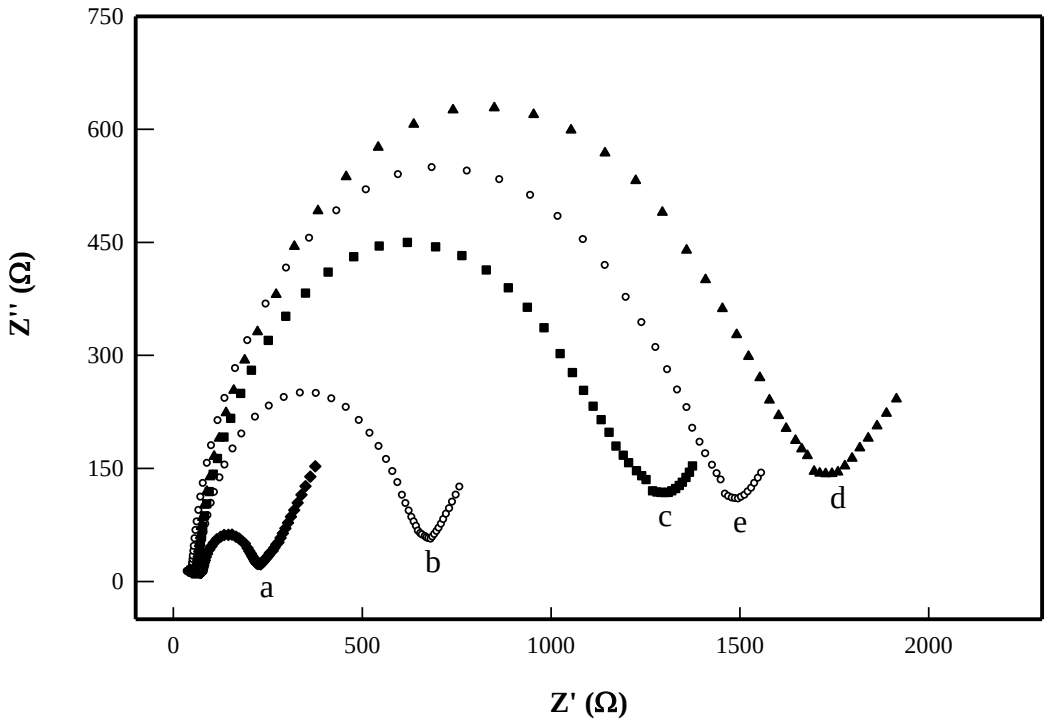

Figure 4. Nyquist plots of (a) MSA–PANI/MWCNTs/GCE, (b) Ab_1-MSA–PANI/MWCNTs/GCE, (c) BSA/Ab_1-MSA–PANI/MWCNTs/GCE, (d) AFP-Ab_1-MSA–PANI/MWCNTs/GCE, (e) g-C_3N_4 NHs@Au-Ab_2-AFP-Ab_1-MSA–PANI/MWCNTs/GCE in 0.1 M KNO_3 containing 10 mM $K_3[Fe(CN)_6]$/ $K_4[Fe(CN)_6]$. The concentration of AFP was 0.3 ng mL^{-1}.

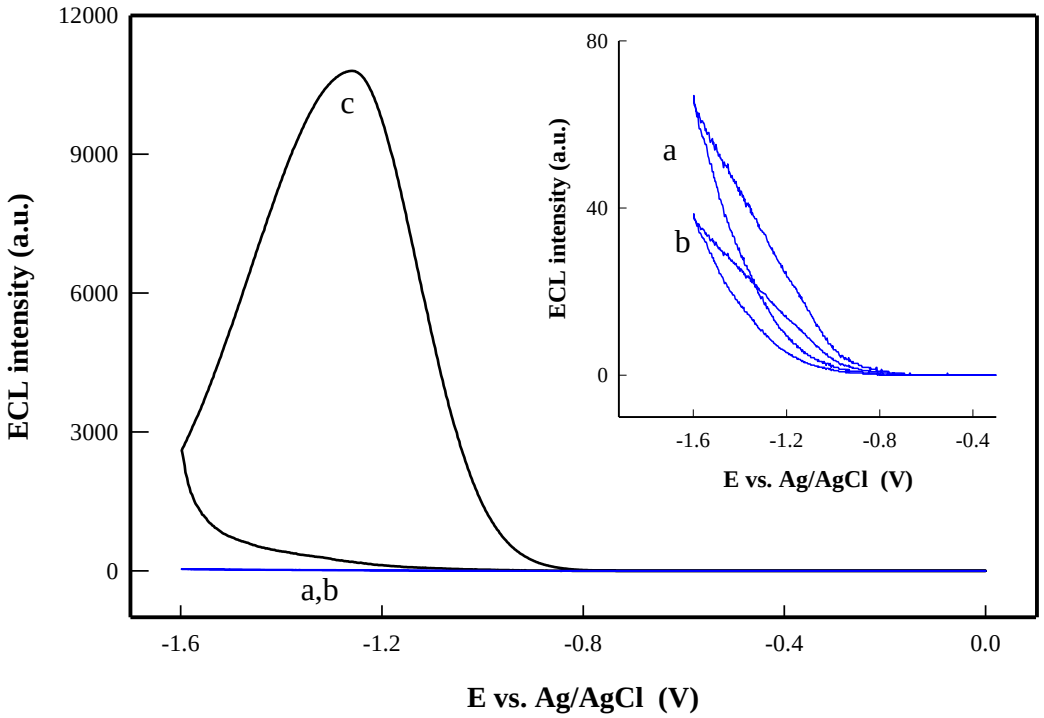

Figure 5. ECL response of (a) MSA–PANI/MWCNTs/GCE, (b) Ab_1MSA–PANI/MWCNTs/GCE, (c) g-C_3N_4 NHs@Au-Ab_2-AFP-Ab_1-MSA-PANI/MWCNTs/GCE in 0.1 M phosphate buffer (pH 7.4) containing 0.1 M $(NH_4)_2S_2O_8$ .The concentration of AFP was 0.3 ng mL^{-1}. The scan rate was 50 mV s^{-1}.

Using the $[Fe(CN)_6]^{3-/4-}$ couple as the redox probe, the EIS spectra of different modified electrodes are depicted in Figure 4. The semicircle diameter of the Nyquist plot indicates the conductivity of electrode or the electron transfer resistance, R_{et}, which controls the electron transfer kinetics of the redox-probe at the electrode interface. It can be seen that the MSA-PANI/ MWCNTs/ GCE exhibits a small semicircle domain with R_{et} = 61 Ω, indicating a faster electron transfer process in this electrode. When Ab_1 was immobilized, the antibodies hindered the electron transfer, resulting in a significant increment of semicircle domain (R_{et} = 216 Ω, curve b). The adsorption of BSA on Ab1/ MSA-PANI/MWCNTs/GCE (R_{et}= 443 Ω, curve c) and the recognition to target antigen (R_{et}=607 Ω, curve d) hindered the electron transfer process further, because the protein layers have low electronic conductivity. After forming the sandwich-type immunocomplex, the electron transfer resistance in g-C_3N_4 NSs@Au- Ab_2-Ab_1/MSA-PANI/MWCNTs/GCE was reduced slightly (R_{et} = 539 Ω, curve e). The reason may be that Au NPs@g-C_3N_4 NSs nanocomposites in the sandwich type immunocomplex can promote the electron transfer process. Importantly, the relative smaller R_{et} value is helpful to enhance the ECL intensity. As reported by Lu and co-workers [39], with increasing concentration of thrombin in a bi-functionalized aptasensor with CdSe quantum dots as the ECL luminophore, the R_{et} value is increased from 2 kΩ to 12 kΩ whiles the ECL intensity was reduced from 500 to 100. Similar correlation between R_{et} value and ECL intensity was observed in a signal-on aptamer-based biosensor for adenosine triphosphate detection using graphene oxide both as an ESI and ECL signal indicator

[40]. For example, with the R_{et} value decreasing from 2.4 kΩ to 0.4 kΩ, the ECL intensity was increased from 250 to 3000.

Figure 5 exhibits the ECL-potential profiles of the resulting signal-on immunosensor. Without the ECL luminophore of g-C_3N_4, only weak ECL was observed (inset). The weak ECL background may be due to the cathodic ECL from $S_2O_8^{2-}$. After the immunological recognition, the g-C_3N_4 NSs in the immunocomplex exhibited strong ECL signal, revealing that the signal-on ECL immunosensor was successfully fabricated. The strong ECL intensity may attribute to the excellent ECL performance of g-C_3N_4 NSs in nanocomposite as well as the small R_{et} value in the MSA-PANI/MWCNTs/GCE. Under the experimental condition used, the ECL onset potential is about -0.83 V and peak potential is at -1.25 V and the ECL peak is in a well symmetrical shape. The high ECL signal from g-C_3N_4 NSs provides a useful platform for immunoassay.

3.3 Optimization of experimental conditions

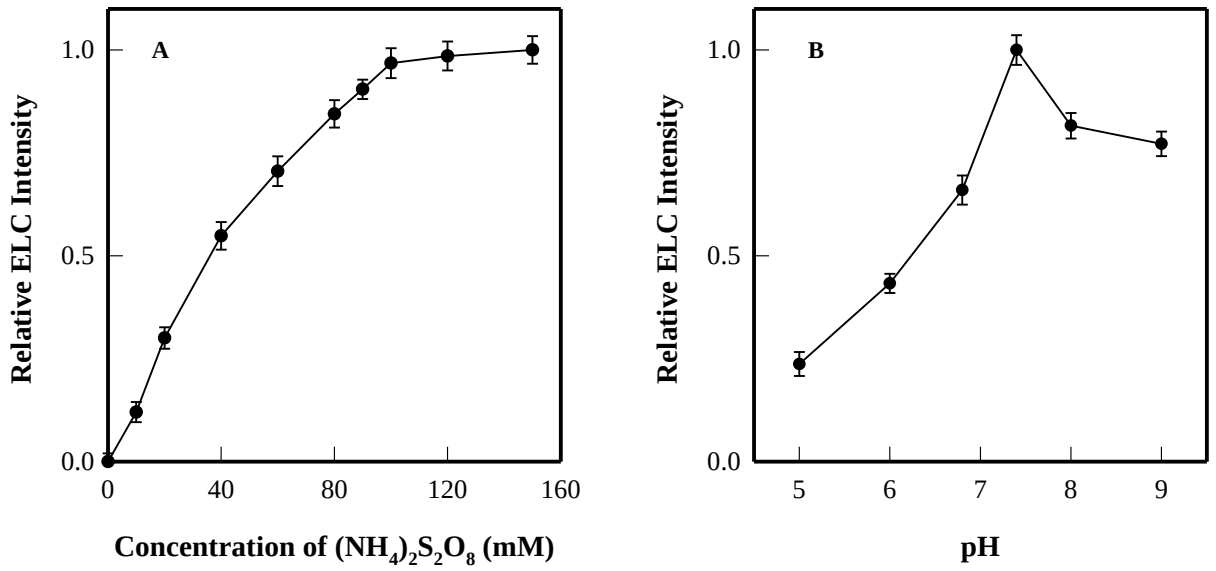

Figure 6. Influence of concentration of $(NH_4)_2S_2O_8$ (A) and pH (B) on the ECL signal of the immunosensor. The concentration of AFP was 0.3 ng mL^{-1}

To achieve an optimal ECL response, the dependence of the concentration of coreactant and pH on the ECL intensity was investigated. g-C_3N_4 is an indirect semiconductor with a medium band gap of about 2.7 eV [41]. The ECL of g-C_3N_4 depends greatly on the coreactant. As shown in Figure 6A, without the coreactant of $(NH_4)_2S_2O_8$, the resulting immunosensor has no ECL signal. With increasing concentration of $(NH_4)_2S_2O_8$, the ECL intensity is enhanced and approached to a stable level with concentration up to 0.1 M. The possible ECL process is given by [26]:

$$g\text{-}C_3N_4 + e \longrightarrow g\text{-}C_3N_4^{\bullet -}$$

$$S_2O_8^{2-} + e \longrightarrow SO_4^{\bullet -} + SO_4^{2-}$$

$$g\text{-}C_3N_4^{\bullet -} + SO_4^{\bullet -} \longrightarrow g\text{-}C_3N_4^{*} + SO_4^{2-}$$

$$g\text{-}C_3N_4^{*} \longrightarrow g\text{-}C_3N_4 + h\nu$$

As can be seen in Figure 6B, the ECL intensity achieved the maximum at pH 7.4. The reason may be that this pH is employed in immune recognition reaction and is favourable for the stability of the sandwich type immunocomplex. In addition, the ECL of g-C_3N_4 NSs themselves is also pH dependent [29]. Hence, the ECL measurements were performed in 0.1 M $(NH_4)_2S_2O_8$ prepared by 0.1 M phosphate buffer of pH 7.4.

3.4 Performance of the immunosensor

The dependence of ECL intensity on the concentration of target antigen of AFP is shown in Figure 7. As a signal-on ECL immunosensor, the ECL intensity is increased gradually with increasing AFP concentration. Under the experimental conditions used, the ECL signal was linear with the logarithm of APF concentration in the range from 0.1 pg mL^{-1} to 1 ng ml^{-1}. Using the signal-to-noise ratio of 3, the limit of detection was estimated to be 0.03 pg mL^{-1}, which is obviously lower than that in a signal-off ECL immunosensor based on g-C_3N_4 NSs (0.5 pg mL^{-1}) [32]. For APF determination, the comparison of the analytical performance of some typical immunoassay methods is summarized in Table 1. It can be seen that the developed signal-on ECL immunosensor offers higher sensitivity, which is beneficial in the practical applications in detecting AFP.

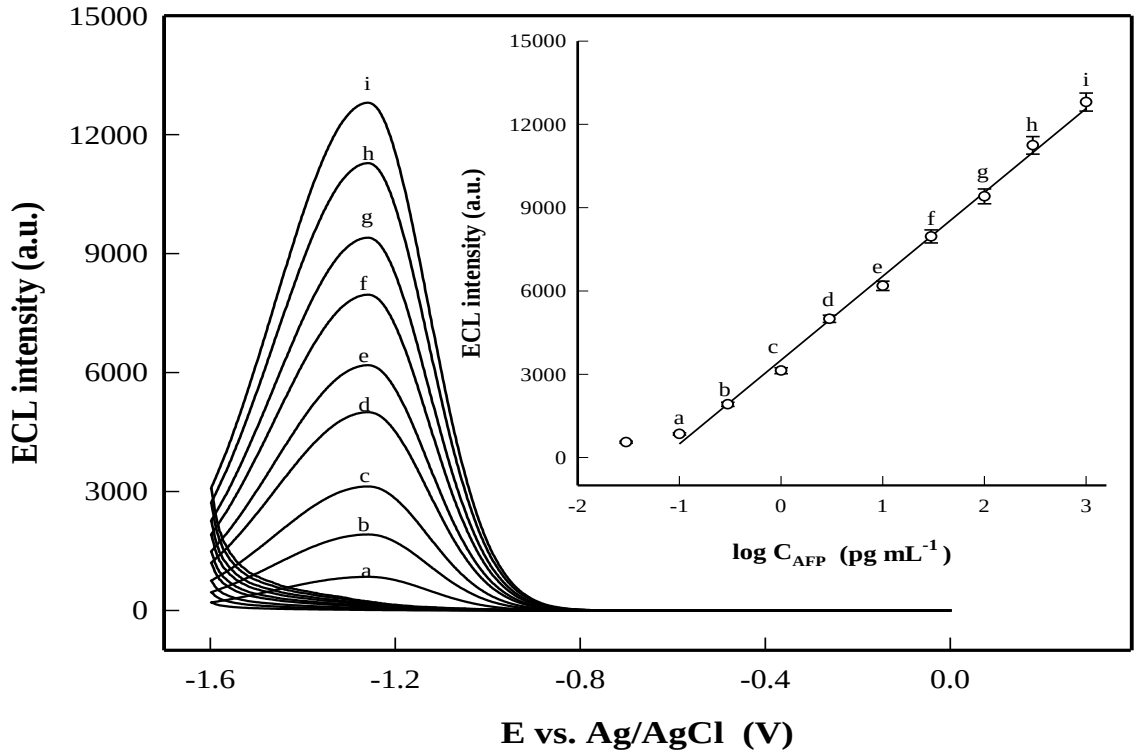

Figure 7. The ECL response of the immunosensor to different concentration of AFP. Insert: Calibration curve in semilogarithmic coordinates. The concentration of AFP in curves *a*→*i* is pointed in insert.

3.5 Reproducibility stability and specificity of the ECL immunosensor

The reproducibility and stability of an immunosensor are important aspects for its practical application. Figure 8A shows the ECL signals of the immunosensor under continuously cyclic potential scanning. The relative standard deviation (RSD) for ten replicate measurements is 0.9%, indicating good stability of the ECL intensity. For five immunosensors prepared independently at the identical experimental conditions, the RSD of the ECL responses to 100 pM AFP is 5.3 %, implying an acceptable reproducibility.

Specificity is an important criterion for biosensors, it played an important role in analyzing biological samples. To test the selectivity of the proposed ECL immunosensor, the ECL response to two typical interfering spices, CEA and hIgG at the concentration of 1ng mL^{-1} was measured. As can be seen in Figure 8B, the ECL intensity is slightly larger than the blank but much less than that with AFP at the concentration of 100 pg mL^{-1}. On the other hand, the ECL response to the mixture of 100pg mL^{-1} AFP + 1ng mL^{-1} CEA + 1ng mL^{-1} hIgG is close to that to 100 pg mL^{-1} AFP. These results indicate that the developed ECL immuosensor offers a good specificity to AFP.

Table 1. Comparison of the analytical performance of some immunoassay methods for AFP determination.

Methods	Signal labels	Signal tag	Linear range ng mL^{-1}	LOD ng mL^{-1}	References
ICP-MS	Ab2-Yb	Yb	0.5–35	0.2	[42]
Colorimetric	SA-HRP	TMB +H_2O_2	0.005-1	0.002	[43]
Fluorescent	Ab2-CuO	Cu^{2+}	1-80	0.45	[44]
fluorescent	Ab2-CuO	Cu^{2+}	0.03–5	0.01	[45]
PEC	Ab2-Bio-APOAA	AA	0.001-1000	3×10^{-4}	[46]
DPV	Ab2-Si@AuNPs-Azure A	Azure A	0.01-25	0.003	[47]
DPV	Ab2-FeC-AuNPs-MPS	FeC	0.5-100	0.1	[48]
DVP	MIP	signal-off	$0.8\text{-}1\times10^{4}$	0.1	[49]
ECL	Ab2-NH_2-G	signal-off	0.01-100	0.003	[40]
ECL	AuNPs-g-C_3N_4	signal-off	0.001-5	5×10^{-4}	[32]
ECL	Ab2-AuNPs-g-C_3N_4	g-C_3N_4	0.0001-1	3×10^{-5}	This work

AA: ascorbic acid, Bio-APOAA: biotin functionalized apoferritin encapsulated ascorbic acid, DPV: differential pulse voltammetry, FeC: 6-ferrocenylhexanethiol, ICP-MS: inductively coupled plasma mass spectrometry, MIP: molecularly imprinted polymer, MPS: mesoporous silica, NH_2-G: aminated grapheme, PEC: photoelectrochemical, SA-HRP: streptavidin-horseradish peroxidase, TMB: 3,30,5,50-tetramethylbenzidine.

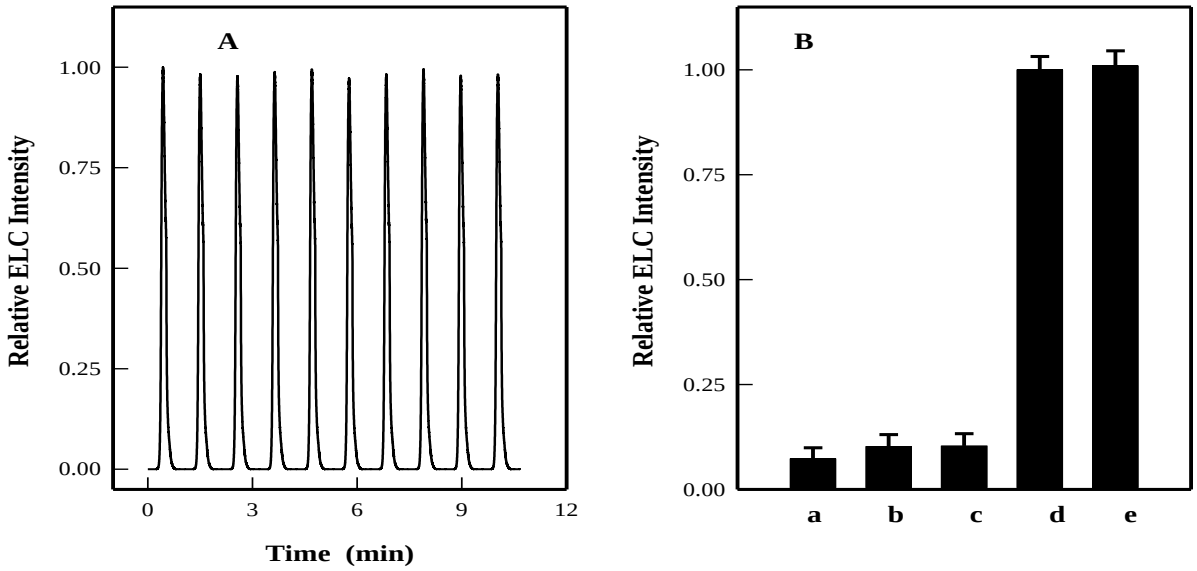

Figure 8. (A) Stability of ECL emissions from Au NPs@ g-C_3N_4 NSs in immunosensor to 3 pg mL^{-1} AFP under 10 continuous CV cycles. (B) The ECL response of the biosensor to different samples: (a) blank, (b) CEA (1 ng mL^{-1}), (c) hIg G (1 ng mL^{-1}), (d) AFP (100 pg mL^{-1}), (e) (b)+(c)+(d).

3.6 Application in analysis of serum sample

The reliability of this immunoassay method was examined by detecting AFP in practical samples. The contents of AFP in three human serum samples were determined for five times. As listed in Table 2. The results determined by present method are in good correlated with those of clinical analyses obtained by the standard ELISA method, implying its promising potential in clinical applications in detection of cancer biomarkers.

Table 2. Comparison of assay results of AFP concentration in in human serum samples from ECLIA with the proposed method.

Samples	Proposed method ng mL^{-1}	ELISA method ng mL^{-1}	Relative deviation %
1	2.79 ± 0.22	2.63	-6.1
2	6.15 ± 0.37	6.71	8.3
3	10.3 ± 0.63	10.9	5.5

4. CONCLUSION

This work clearly demonstrates that Au NPs@g-C_3N_4 NSs is a promising ECL luminophore for signal-on immunosensors, offering high sensitivity, selectivity and reproducibility due to good

biocompatibility, large surface area and the high ECL intensity of the nanocomposite. Au NPs in Au NPs@ g-C_3N_4 NSs can be serviced as the support to immobilize signal antibody and enhance the ECL intensity of g-C_3N_4 to promote the detection sensitivity. The good stability of Au NPs@g-C_3N_4 NSs extends the promising applications in ECL biosensing. The modified electrode of MSA–PANI/MWCNTs/GCE is a useful platform for capture probe immobilization with high electrical conductivity. The proposed signal-on ECL immunosensor shows a wide linear response range and a low LOD of 0.03 pg mL^{-1} for AFP. Such protocol exhibited high sensitivity, good stability and promising applications in clinical analysis.

ACKNOWLEDGEMENTS
The authors gratefully acknowledge financial support of National Natural Science Foundation of China (21575080, 21275091, 21175084).

References

1. L. Wu, X.G. Qu, *Chem. Soc. Rev.*,44(2015)2963.
2. S. Mittal, H. Kaur, N. Gautam, A.K. Mantha, *Biosens. Bioelectron.*,88(2017)217.
3. A.P.F. Turner, *Chem. Soc. Rev.*, 42(2013) 3184.
4. S.M. Ling, Q.A. Chen, Y.M. Zhang, R.Z. Wang, N. Jin, J. Pang, S.H. Wang, *Biosens. Bioelectron.*, 71 (2015)256.
5. E. Mauriz, M.C. García-Fernández, L.M. Lechuga, *Trends Anal. Chem.*, 79 (2016)191.
6. M. Hu, J. Yan, Y. He, H.T. Lu, L.X. Weng, S.P. Song, C.H. Fan, L.H. Wang, *ACS Nano*, 4(2016)488.
7. F. Chen, H.L.Li, J.L.Yan, H.M.Guo, Y.F.Tu, *ChemElectroChem*, 4(2017)1.
8. W.Y. Gao, M. Saqib, L.M. Qi, W. Zhang, G.B. Xu, *Current Opin. Electrochem.*, 000(2017)1.
9. J.W. Sun, H. Sun, Z.Q. Liang, *ChemElectroChem*, 4(2017)1.
10. P. Chikhaliwala, S. Chandra, *J.Organometal. Chem.*, 821 (2016) 78.
11. K.Y. Yi, C.S. Wei, *Int. J. Electrochem. Sci.*, 12 (2017)3472.
12. X.L. Ma, X. Zhang, X.L.Guo, Q. Kang, D.Z. Shen, G.Z. Zou, *Talanta*, 154(2016)175.
13. Y.H. Xu, J.Q. Liu, C.L. Gao, E.K.Wang, *Electrochem.Commun.*,48(2014)151.
14. R.B. Xie, Z.F. Wang, W. Zhou, Y.T. Liu, L.Z. Fan, Y.C. Li, X.H. Li, *Anal. Methods*, 8(2016)4001.
15. M.Y. Xiong, Q.M. Rong, H.M. Meng, X.B. Zhang, *Biosens. Bioelectron.*, 89 (2017)212.
16. P. Bollella, G. Fusco, C. Tortolini, G. Sanzò, G. Favero,L. Gorton, R. Antiochia, *Biosens. Bioelectron.*, 89 (2017) 152.
17. Q.Zhang, H. Wang, S. Chen, Y. Su, X. Quan, *RSC Adv.*, 7(2017)13223.
18. Z.Y. Mao, J.J. Chen, Y.F. Yang, D.J. Wang, L.J. Bie, B. D. Fahlman, *ACS Appl. Mater. Interfaces*, 9(2017)12427.
19. M.J. Zhou, Z.H. Hou, L. Zhang, Y. Liu, Q.Z. Gao, X.B. Chen, *Sustain. Energy Fuels*, 1(2017)317.
20. J.Y. Zhuang, W.Q. Lai, M.D. Xu, Q. Zhou, D.P. Tang, *ACS Appl. Mater. Interfaces*, 7(2015)8330.
21. H.S. Yin, B. Sun, L.F. Dong, B.C. Li, Y.L. Zhou, S.Y. Ai, *Biosens. Bioelectron.*,64 (2015) 462.
22. Q. Kang, X.X. Wang, X.L. Ma, L.Q.Kong, P. Zhang, D.Z. Shen, *Sens. Actuators B*,228(2016)565.
23. F. Tian, J Lyu, J.Y Shi, M. Yang, *Biosens. Bioelectron.*,89(2017)123.
24. M.Y. Xiong, Q.M. Rong, H.M. Meng, X.B. Zhang, *Biosens. Bioelectron.*,89(2017)212.
25. C.M.Cheng, Y. Huang, X.Q. Tian, B.Z. Zheng, Y. Li, H.Y. Yuan,D. Xiao, S.P. Xie, M. M. F. Choi, *Anal. Chem.*, 84(2012)4754.
26. C.M. Cheng, Y. Huang, J. Wang, B.Z. Zheng, H.Y. Yuan, D. Xiao, *Anal. Chem.*, 85(2013) 2601.

27. N.Y. Cheng, P. Jiang, Q. Liu, J.Q. Tian, A. M. Asiri, X.P. Sun, *Analyst*, 139(2014) 5065.
28. Q.Y. Lu, J.J. Zhang, X.F. Liu, Y.Y. Wu, R. Yuan, S.H. Chen, *Analyst*, 139(2014)6556.
29. B.X. Wang, H.J. Wang, X. Zhong, Y.Q. Chai, S.H. Chen, R. Yuan, *Chem. Commun.*, 52(2016) 5049.
30. S.H. Chen, A.M. Li, L.Z. Zhang, J.M. Gong, *Anal. Chim. Acta*, 896 (2015) 68.
31. J.J. Xu, D.P. Jiang, Y.L. Qin, J. Xia, D.C. Jiang, H.Y. Chen, Anal. Chem., 89(2017)2216.
32. X.L. Zheng, X.X. Hua, X.Y. Qiao, F.Q. Xia, D. Tian, C.L. Zhou, *RSC Adv.*, 6(2016) 21308.
33. L.C. Chen, X.T. Zeng, P. Si, Y.M. Chen, Y.W. Chi, D.H. Kim, G.N. Chen, *Anal. Chem.*, 86(2014)4188.
34. Y.Z. Wang, N. Hao, Q.M. Feng, H.W. Shi, J.J. Xu, H.Y. Chen, *Biosens. Bioelectron.*,77(2016)76.
35. X. Ou, X.R. Tan, X.F. Liu, Q.Y. Lu , S.H. Chen, S.P. Wei, *Biosens. Bioelectron.*, 70 (2015) 89.
36. Z.Y. Guo, L. Wu, Y.F. Hu, S. Wang, X. Li, *Biosens. Bioelectron.*,95 (2017) 27.
37. H.F. Xu, S.J. Liang, X. Zhu, X.Q. Wu, Y.Q. Dong, H.S. Wu, W.X. Zhang, Y.W. Chi, *Biosens. Bioelectron.*,92(2017) 695.
38. Y.Liu, Z.H. Su, Y. Zhang, L. Chen, T.A. Gu, S.Y. Huang,Y. Liu, L.G. Sun ,Q.J. Xie , S.Z. Yao, *J. Electroanal. Chem.*,709(2013)19.
39. L.P Lu, J. Li, T.F. Kang, S.Y. Cheng,*Talanta*,138 (2015) 273.
40. X. Huang,Y.Q. Li, X.S. Zhang, X. Zhang, Y.W. Chen,W.H. Gao, *Analyst*, 140(2015) 6015.
41. D.R. Miller, D.C. Swenson, E.G. Gillan, *J. Am. Chem. Soc.*,126 (2004) 5372.
42. Z.R. Liu, B. Yang, B.B. Chen, M. He, B. Hu, *Analyst*, 142(2017) 197.
43. C.H. Chen, Y.F. Liu, Z.H. Zheng, G.H. Zhou, X.H Ji, H.Z. Wang, Z.K. He, *Anal. Chim. Acta*, 880 (2015) 1.
44. Y.W. Wang, L.Y. Chen, M.F. Liang, H. Xu, S.R. Tang, H.H. Yang , H.B. Song, *Sens.Actuators B*, 247 (2017) 408.
45. Q.F. Xie , X.H. Weng , L.J. Lu , Z.Y. Lin , X.W. Xu , C.L. Fu, *Biosens. Bioelectron.*, 77(2016) 46.
46. J.X. Chen, G. C. Zhao, *Biosens. Bioelectr*on., 98 (2017) 155.
47. J.Q. Zhao ,Z.L. Guo ,D.X. Feng , J.J. Guo ,J.C. Wang ,Y.Z. Zhang, *Microchim. Acta*, 182(2015) 2435.
48. J.H. Lin, H.H. Zhang, S.Y. Niu, *Microchim. Acta*,182 (2015)719.
49. X.L. Shen, Y. Ma, Q. Zeng, J. Tao, J.Z. Huang, L.S. Wang, *Anal. Methods*, 8(2016) 7361.
50. J. Zhou, T.Q. Han, H.M. Ma, T. Yan, X.H. Pang, Y.Y. Li,Q. Wei, *Anal. Chim. Acta*, 889 (2015) 82.